Catalysis of hydrosilylation by well-defined rhodium siloxide complexes immobilized on silica

Bogdan Marciniec [a,*], Karol Szubert [a], Ryszard Fiedorow [a], Ireneusz Kownacki [a], Marek J. Potrzebowski [b], Michał Dutkiewicz [a], Adrian Franczyk [a]

[a] Faculty of Chemistry, Adam Mickiewicz University, Grunwaldzka 6, 60780 Poznan, Poland
[b] Laboratory for Analysis of Organic Compounds and Polymers, Centre of Molecular and Macromolecular Studies,
Polish Academy of Sciences, Sienkiewicza 112, 90-363 Lodz, Poland

ARTICLE INFO

ABSTRACT

Rhodium surface siloxide complexes were prepared directly by condensation of the molecular precursors ($[\{Rh(\mu\text{-OSiMe}_3)(cod)\}_2]$, $[\{Rh(\mu\text{-OSiMe}_3)(tfb)\}_2]$, $[\{Rh(\mu\text{-OSiMe}_3)(nbd)\}_2]$) with silanol groups on silica surface (Aerosil 200 and SBA-15) and their structures were characterized by ^{13}C and ^{29}Si CP/MAS NMR spectroscopy. Such single-site complexes were tested for their activity in hydrosilylation of carbon–carbon double bonds with triethoxysilane, heptamethyltrisiloxane and poly(hydro,methyl)(dimethyl)siloxane. The best catalyst appeared to be cyclooctadiene ligand-containing rhodium siloxide complex immobilized on Aerosil which was recycled as many as 20 times without loss of activity and selectivity in hydrosilylation of vinylheptamethyltrisiloxane with heptamethyltrisiloxane. On the ground of CP/MAS NMR measurements it was established that the mechanism of hydrosilylation catalyzed by silica-supported rhodium siloxide complexes is different from that for the complexes in the homogeneous system.

© 2009 Elsevier B.V. All rights reserved.

1. Introduction

Transition metal siloxide complexes including terminal and/or bridging siloxy ligands are regarded as a good molecular model of metal complexes immobilized on silica surface [1–3]. The properties of siloxide as ancillary ligand in the system TM-O-SiR$_3$ have been used in molecular catalysis but predominantly in the case of early transition metal complexes, i.e. Ti, W, V which can be effectively applied to polymerization [4], metathesis [5] and epoxidation [6] of alkenes as well as dehydrogenative coupling of silanes [7]. Since 1995 our work (as well as some other groups) has been focused on the study of well-defined binuclear and mononuclear rhodium [8–12] and iridium complexes [13–15], their synthesis, structure, reactivity and application to homogeneous catalysis in organosilicon chemistry. Siloxide rhodium complexes, particularly binuclear ones with siloxide bridged ligand, appeared to be much more effective than the respective chlorocomplex (as well as the commercially available Pt-Karstedt catalyst) in hydrosilylation of a variety of olefins such as 1-hexene [16], vinylsilanes [17] and allyl alkyl ethers [18,19] (for recent review see [20]) as well as in the silylative coupling [21,22] and hydroformylation of vinylsilanes [23].

Surface rhodium-siloxy complexes have been of great interest since 1980 when Basset and Ugo groups [24] proposed a formulation of the oxidized species with Rh(CO) moieties bonded to the support by SiO bond which was confirmed by the IR characterization of $[Rh(\mu\text{-OSiMe}_3)(CO)_2]_2$. Next experimental study on the reaction of $[Rh(\eta^3\text{-}C_3H_5)_3]$ with the surface hydroxyl group of partially dehydroxylated silica enabled a synthesis of well-defined surface organometallic complexes [25,26]. As a result three surface rhodium fragments were characterized (see Fig. 1).

However, although those complexes were tested for their performance in catalytic reactions, no results have been published yet on their efficiency in recycling tests [25,26].

As a continuation of our experience with soluble rhodium and iridium siloxide complexes, our recent studies are focused on immobilization of organometallic rhodium derivatives on silica surface and their application to catalysis. We reported the synthesis and characterization of silica-supported well-defined rhodium siloxide complexes obtained directly by the reaction of molecular rhodium siloxide precursors with silanol groups of silica surface as shown in Fig. 2 [27–29].

Preliminary results on catalytic activity for the hydrosilylation of 1-alkenes and vinylsiloxanes by heptamethyltrisiloxane were reported to illustrate their high efficiency in recycling tests [27].

The aim of this paper is to present a full picture of the surface rhodium siloxide complexes as effective catalysts for hydrosilylation of olefins as commercially important pro-
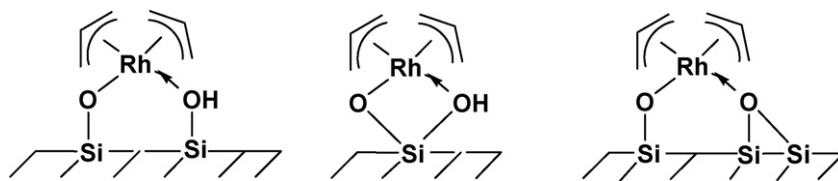
Fig. 1. Structures of rhodium π-allyl complexes immobilized on silica.

cesses. For recent advances in catalytic hydrosilylation see Ref. [30].

2. Experimental

All experiments were performed under the dry and oxygen-free argon using standard Schlenk's technique for the organometallic synthesis. Rhodium complexes [{Rh(μ-OSiMe$_3$)(cod)}$_2$], [{Rh(μ-OSiMe$_3$)(tfb)}$_2$], [{Rh(μ-OSiMe$_3$)(nbd)}$_2$] were prepared as described in Refs. [31–33]. Heptamethyltrisiloxane and poly(hydro,methyl)(dimethyl)siloxane were purchased from Gelest, olefins and other reagents from Aldrich; Aerosil 200 was obtained from Degussa AG.

Mass spectra of the products and substrates were determined by GC–MS (Varian Saturn 2100T equipped with a 30 m DB-1 capillary column). GC analyses were carried out on a Varian 3800 series gas chromatograph with a 30 m DB-1 capillary column and TCD.

The content of rhodium in all catalysts immobilized on the silica surface was measured by Varian Vista-MPX Inductively Coupled Plasma Optical Emission Spectrometer (ICP-OES).

2.1. Solid-state NMR spectroscopy

The solid-state cross-polarization magic angle spinning (CP/MAS) experiments were performed on a Bruker Avance DSX 300 spectrometer at frequency of 75.47 MHz for ^{13}C and 300.13 MHz for proton, equipped with a MAS probe head using 4-mm ZrO$_2$ rotors. A sample of glycine was used for setting the Hartmann–Hahn condition and adamantane was employed as a secondary chemical shift reference $\delta = 38.48$ ppm and 29.46 ppm from external TMS [34]. The conventional spectra were recorded with a proton 90° pulse length of 3.5 μs and a contact time of 1 ms. The repetition delay was 10 s and the spectral width was 25 kHz. The FIDs were accumulated with a time domain size of 2k data points. The RAMP shape pulse [35] was used during the cross-polarization and TPPM decoupling [36] with $\tau_p = 6.8$ μs and the phase angle of 20° during the acquisition. The cross-polarization efficiency was measured in contact times between 10 μs and 12 ms.

The solid-state ^{29}Si CP/MAS NMR spectra were recorded with high-power proton decoupling at 59.62 MHz for ^{29}Si. The number of data points was 2k, magic angle spinning (MAS) frequency was 10 kHz. The number of scans for accumulation was 1k–10k, repetition delay was 30 s and spin lock pulse 0.1–10 ms. ^{29}Si scale was calibrated by the external M$_8$Q$_8$ (-108.9 ppm, the high-

est field signal). The same sample was used for setting ^{1}H–^{29}Si Hartmann–Hahn condition.

2.2. Preparation of SBA-15

SBA-15 was prepared according to a slightly modified procedure described by Stucky et al. [37] using tetraethoxysilane (TEOS) as a source of silicon and a triblock copolymer P123 (Aldrich) as a structure directing agent. 4 g of the latter were mixed with 30 cm^3 of water and 116 cm^3 of 2 M HCl and stirred at 35 °C. When P123 was dissolved, 9.1 cm^3 of TEOS were added, followed by stirring at 35 °C for 20 h, heating at 100 °C without stirring, filtering, washing and air-drying. Then the sample was heated in air to 500 °C and after reaching the above temperature the calcination was continued for 6 h.

2.3. Catalyst preparation and characterization

Surface areas of the silica samples were determined on a sorptometer ASAP 2010 (Micromeritics). Primary particles of Aerosil 200 are nonporous, but their small size (12 nm on the average) results in a relatively large surface area of 202 m^2/g. On the other hand, SBA-15 is a highly ordered mesoporous material with surface area of 891 m^2/g.

Number of silanol groups on 1 nm^2 of the silica supports heated at 350 °C was determined by subjecting them to calcination at 1200 °C for 4 h and calculated from the formula:

$$N_{OH} = \frac{2000W}{3S}$$

where W is the mass loss in % after calcination at 1200 °C and S is the BET surface area in m^2/g [27]. In the case of Aerosil 200, $N_{OH} = 3.8$ and in that of SBA-15 $N_{OH} = 3.0$, i.e. in both cases there is less than one OH group per one silicon atom. When each Si atom on the surface carries one silanol group $N_{OH} = 4.6$ [38].

2.4. Synthesis of complex 1a

1.2 g of di-μ-trimethylsiloxybis{(1,5-cyclooctadiene)rhodium (I)} and 6 g of Aerosil 200 (dried at 350 °C) were placed in a glass two-necked round-bottom flask of 50 mL in capacity, equipped with a magnetic stirrer, in a neutral gas atmosphere. After the addition of 20 mL of pentane, the contents were stirred at room temperature for 24 h. The supernatant solution was decanted and the precipitate
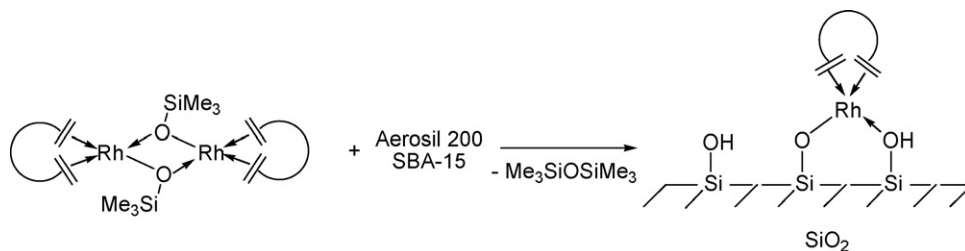

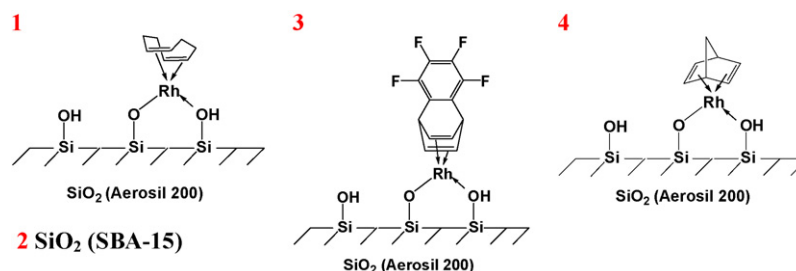**Fig. 2.** Immobilization of rhodium(diene)siloxide complex on silica surface.

Fig. 3. Surface rhodium siloxide complexes **1**–**4**.

was washed three times with pentane and dried under reduced pressure. In this way the catalyst (≡SiO)(≡SiOX)Rh(cod)](Aerosil 200) (where X = H or Si≡) was obtained, rhodium content of which was 2.17×10^{-4} mol Rh/g.

^{13}C CP/MAS NMR (ppm) = 75.19 (=CH–, cod); 31.02 (CH$_2$, cod)

^{29}Si CP/MAS NMR (ppm) = 99.68 (Q^2), 106.88 (Q^3), 110.38 (Q^4)

2.5. Synthesis of complex **1b**

1.2 g of di-μ-trimethylsiloxybis{(1,5-cyclooctadiene)rhodium (I)} and 6 g of Aerosil 200 (dried at 350 °C) were placed in a glass two-necked round-bottom flask of 50 mL in capacity, equipped with a magnetic stirrer, in a neutral gas atmosphere. After addition of 20 mL of benzene, the contents were stirred at room temperature for 24 h. Then, benzene was evaporated under reduced pressure and 20 mL of pentane was added. The supernatant solution was decanted and the precipitate was washed three times with pentane and dried under reduced pressure. The above procedure resulted in the catalyst [(≡SiO)(≡SiOX)Rh(cod)](Aerosil 200) which contained 4.10×10^{-4} mol Rh/g.

^{13}C CP/MAS NMR (ppm) = 75.19 (=CH–, cod); 31.02 (CH$_2$, cod)

^{29}Si CP/MAS NMR (ppm) = 99.68 (Q^2), 106.88 (Q^3), 110.38 (Q^4)

2.6. Synthesis of complex **2**

Complex **2** was synthesized according to the procedure described for complex **1a**, except for the fact that 1.3 g of di-μ-trimethylsiloxybis{(1,5-cyclooctadiene)rhodium(I)} and 2 g of SBA-15 (dried at 350 °C) were used. The catalyst obtained was [(≡SiO)(≡SiOX)Rh(cod)](SBA-15) and its rhodium content was 8.13×10^{-4} mol Rh/g.

^{13}C CP/MAS NMR (ppm)

= 85.24, 75.19 (=CH–, cod); 29.28 (CH$_2$, cod)

^{29}Si CP/MAS NMR (ppm) = 101.02 (Q^2), 105.73 (Q^3), 108.87 (Q^4)

2.7. Synthesis of complex **3**

Complex **3** was synthesized according to the procedure described for complex **1a**, except for the fact that 1.33 g of di-μ-trimethylsiloxybis {(tetrafluorobenzobarrelene)rhodium(I)} and 5 g of Aerosil 200 were used. The catalyst obtained was [(≡SiO)(≡SiOX)Rh(tfb)](Aerosil 200) and it contained 2.32×10^{-4} mol Rh/g.

^{13}C CP/MAS NMR (ppm)

= 138.18, 125.50 (=CH–, tfb); 47.84, 39.47 (CH, tfb)

^{29}Si CP/MAS NMR (ppm) = 99.74 (Q^2), 106.78 (Q^3), 110.31 (Q^4)

2.8. Synthesis of complex **4**

Complex **4** was synthesized according to the procedure described for complex **1a**, except for the fact that 1.2 g of di-μ-trimethylsiloxybis{(norbornadiene)rhodium(I)} and 6.5 g of Aerosil 200 were used. The catalyst obtained was (≡SiO)(≡SiOX)Rh(nbd)](Aerosil 200) of rhodium content 5.00×10^{-4} mol Rh/g.

^{13}C CP/MAS NMR (ppm) = 60.57 (=CH–, nbd); 46.54 (–CH$_2$–, nbd)

^{29}Si CP/MAS NMR (ppm) = 99.77 (Q^2), 106.68 (Q^3), 110.33 (Q^4)

2.9. Catalytic activity tests

In a reactor equipped with a reflux condenser and a stirrer, a portion of complexes **1**–**4** (5×10^{-6} mol of Rh) was placed in argon atmosphere, followed by the addition of silane or (poly)siloxane (5×10^{-2} mol) and terminal olefin (5×10^{-2} mol). The reaction mixture was heated for 1 h at 100 °C and then catalyst was separated from the raw product by decantation. After the removal of the raw product, a new portion of substrates was added and the reaction was repeated in the same conditions.

Table 1
NMR data of catalysts **1**–**4**.

1	2	3	4
^{13}C CP/MAS			
74.89 (=CH–, cod); 29.20 (–CH$_2$–, cod)	85.23, 74.11 (=CH–, cod); 28.60 (–CH$_2$–, cod)	137.97, 125.52 (=CH–, tfb); 46.94, 38.82 (CH, tfb)	60.57 (=CH–, nbd); 48.52 (–CH$_2$–, nbd)
^{29}Si CP/MAS			
101.84 (Q^2), 105.30 (Q^3), 108.35 (Q^4)	102.16 (Q^2), 105.83 (Q^3), 109.11 (Q^4)	99.48 (Q^2), 103.91 (Q^3), 106.19 (Q^4)	100.68 (Q^2), 106.19 (Q^3)

3. Results and discussion

A series of rhodium-modified heterogeneous materials was prepared [28,29] using two silicon dioxide samples (Aerosil 200 and SBA-15) and dinuclear rhodium(I) siloxide precursors [{Rh(μ-OSiMe$_3$)(cod)}$_2$], [{Rh(μ-OSiMe$_3$)(nbd)}$_2$], [{Rh(μ-OSiMe$_3$)(tfb)}$_2$] (see Fig. 3). The difference in synthesis of complexes **1a** and **1b** consists in solvent (pentane – complex **1a** and benzene – complex **1b**) used in the reaction.

Structures of immobilized rhodium complexes on silica support were proposed on the basis of the data obtained from ^{13}C and ^{29}Si CP/MAS NMR measurements. NMR spectra of the rhodium-modified solid materials confirmed that trimethylsiloxide ligand was removed from the rhodium coordination sphere during the immobilization process. Formation of a new covalent bond between the rhodium organometallic moiety and the silica support occurs probably with evolution of trimethylsilanol, which is rapidly converted to disiloxane (Me$_3$Si)$_2$O. The presence of this molecule in the solution obtained after silica surface modification process was confirmed by GC–MS analysis.
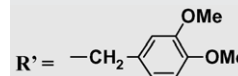
^{13}C and ^{29}Si CP/MAS NMR spectra of catalysts **1–4** have shown characteristic signals assigned to structural fragments of rhodium organometallic moiety attached to the inorganic support (see Table 1).

Selected well-defined silica-supported heterogeneous rhodium catalysts **1–5** were tested for their performance in conversion of organosilicon compounds, i.e. hydrosilylation of olefins with HSi(OEt)$_3$ [39], heptamethyltrisiloxane and polyhydrosiloxane [40,41].

The catalytic results, compiled in Table 2, show high effectiveness of catalyst **1b** investigated in hydrosilylation of exemplary terminal olefins, namely 1-hexene, 1-hexadecene (1-C$_{16}$H$_{32}$) and 2,4-dimethoxyallylbenzene, with heptamethyltrisiloxane (HMTS) and poly(hydro,methyl)(dimethyl)siloxane. The catalysts were subjected to recycling tests.

Table 2
Hydrosilylation of 1-hexene, 1-hexadecene and 2,4-dimethoxyallylbenzene with substituted silanes and (poly)siloxanes, catalyzed by complex **1b**. R$_3$SiH + H$_2$C = CHR' $\xrightarrow{[Rh]}$ R$_3$SiCH$_2$CH$_2$R'.

R$_3$SiH	Yield (%)
R' = –(CH$_2$)$_{13}$CH$_3$	
Heptamethyltrisiloxane	97 (TOF = 162 min^{-1}) (97, 92, 98, 98, 92, 96, 92, 94, 95, 94, 93, 90, 90, 88)
Poly(hydro,methyl)(dimethyl)siloxane	99 (99, 99, 99, 99, 99, 99, 99, 99, 99)
R' = –(CH$_2$)$_3$CH$_3$ [a]	
Heptamethyltrisiloxane	97 (97, 93, 98, 98, 93, 87, 83, 85, 95, 85, 77, 64, 60, 87)
Poly(hydro,methyl)(dimethyl)siloxane	99 (99, 99, 99, 99, 99, 99, 99, 99, 99)
R' = –CH$_2$–C$_6$H$_3$(OMe)$_2$ (2,4-OMe)	
Heptamethyltrisiloxane	90 (TOF = 150 min^{-1}) (90, 82, 98, 97, 97, 96, 82, 66, 60)
Poly(hydro,methyl)(dimethyl)siloxane	99 (99, 99, 99, 99, 99, 99, 99, 90, 75)

Reaction conditions—[SiH]:[H$_2$C=CHR]:[Rh] = 1:1:10^{-4}, T = 100 °C, 1 h, open system, glass ampoules, argon.
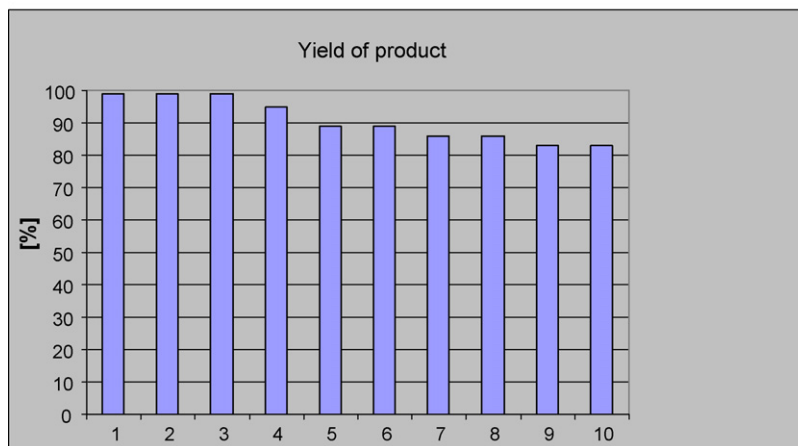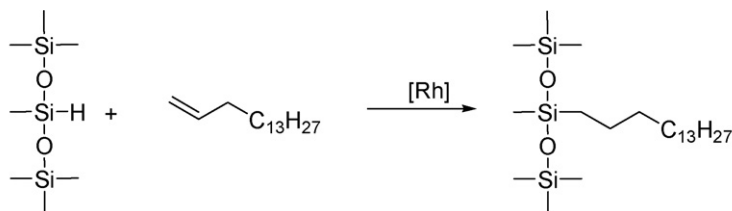
[a] Reaction catalyzed by complex **1a**.

After completion of each reaction cycle, the post-reaction mixture was decanted and the catalyst left on the bottom of the reaction vessel was used in subsequent runs. In most of reactions studied, the catalytic activity remained practically unchanged for over 10 runs (Figs. 4 and 5).

In order to compare catalytic activity of all **1–4** catalysts for hydrosilylation, the molecular model of cross-linking reaction of silicones was used as a test reaction (Table 3).

The surface complex **1** has appeared to be the most effective catalyst for hydrosilylation of vinylheptamethyltrisiloxane (VHMTS)
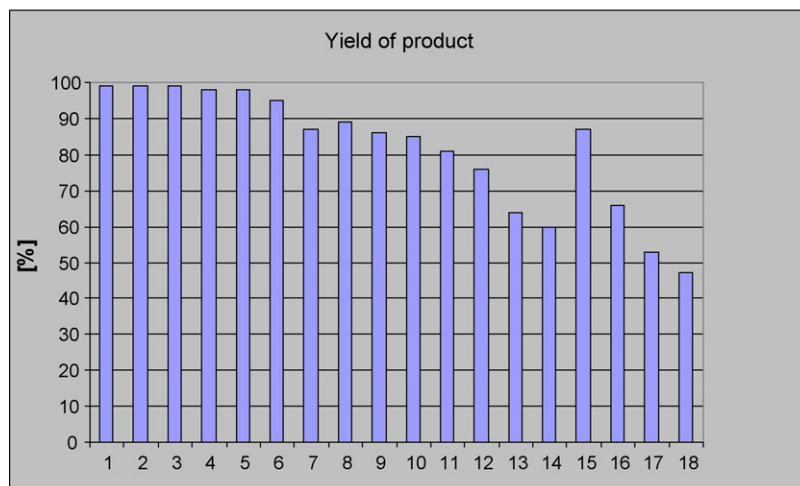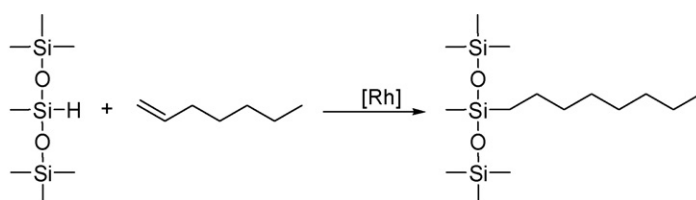

Fig. 4. Hydrosilylation of 1-hexene by heptamethyltrisiloxane catalyzed by complex **2**. Reaction conditions—[SiH]:[H$_2$C=CHR]:[Rh] = 1:1:10^{-4}, T = 100 °C, 1 h, open system, glass ampoules, argon.

Fig. 5. Hydrosilylation of 1-hexedecene by heptamethyltrisiloxane catalyzed by complex **4**. Reaction conditions—[SiH]:[H$_2$C=CHR]:[Rh] = 1:1:10^{-4}, T = 100 °C, 1 h, open system, glass ampoules, argon.

Table 3
Hydrosilylation of vinylheptamethyltrisiloxane by heptamethyltrisiloxane.
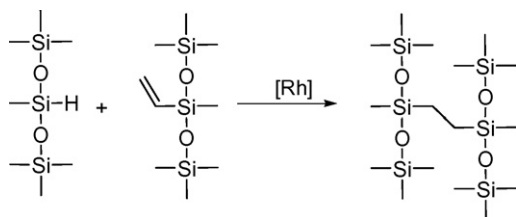
Cat.	Yield (%)
1a	88 (86, 86, 88, 87, 86, 86, 86, 86, 86, 85, 82, 83, 82, 81, 79, 80, 80, 80, 80)
1b	88 (TOF = 150 min^{-1}) (86, 86, 88, 90, 88, 88, 88, 88, 86, 85, 83, 83, 83, 83, 84, 84, 84, 86, 86)
2	90 (89, 91, 79, 86, 86, 87, 86, 86, 51, 56, 56, 56, 58, 58, 58, 58, 57, 58, 58, 56)
3	89 (88, 85, 80, 78, 70, 70, 70, 69, 69)
4	92 (92, 92, 90, 90, 90, 90, 89, 89, 88)

Reaction conditions—[SiH]:[H$_2$C=CHR]:[Rh] = 1:1:10^{-4}, T = 100 °C, 1 h, open system, glass ampoules, argon.
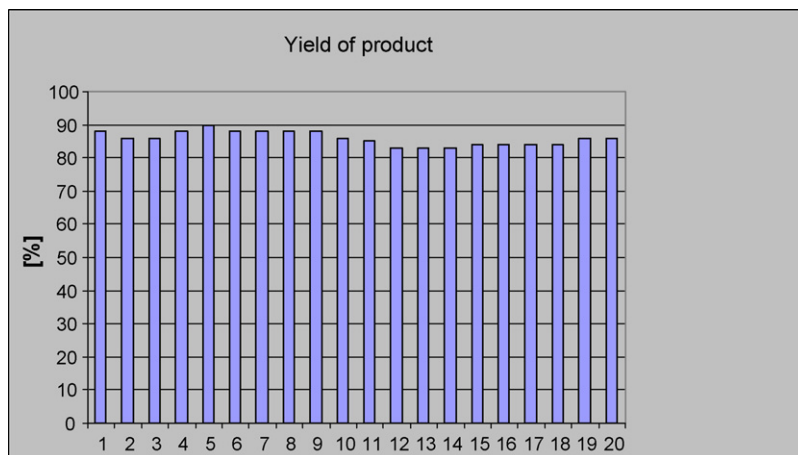
Fig. 6. Hydrosilylation of vinylheptamethyltrisiloxane with heptamethyltrisiloxane catalyzed by complex **1b**. Reaction conditions—[SiH]:[H$_2$C=CHR]:[Rh] = 1:1:10^{-4}, T = 100 °C, 1 h, open system, glass ampoules, argon.
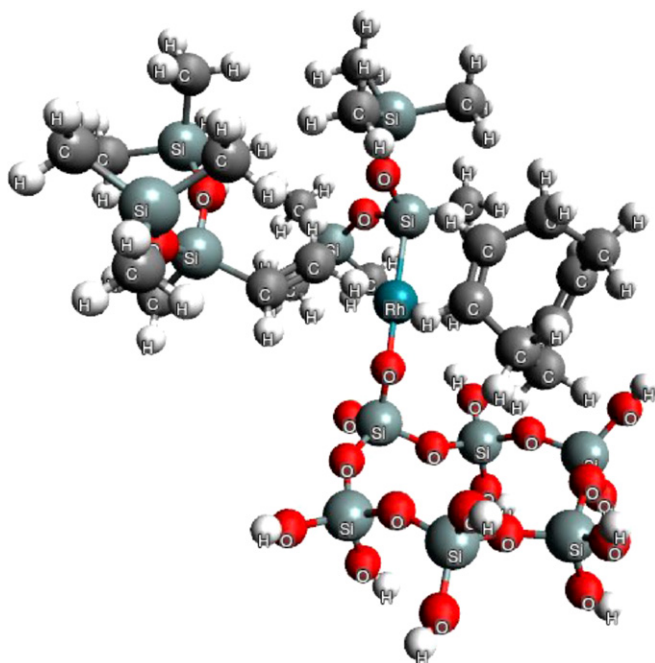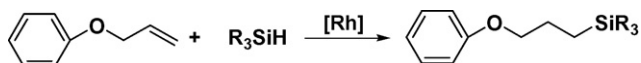
Fig. 7. Activated complex **6** (see Fig. 10, where HSiR$_3$ = HMTS and H$_2$C=CHR' = VHMTS) optimized by the UFF method.

Table 4

Hydrosilylation of allyl phenyl ether by substituted silanes and (poly)siloxanes.

Cat.	Yield (%)
Triethoxysilane	
1b	92 (92, 92, 92, 91, 89, 50, 62)
Heptamethyltrisiloxane	
1b	80 (TOF = 133 min^{-1}) (76, 76, 76, 79, 85, 82, 88, 88, 87)
3	84
Poly(hydro,methyl)(dimethyl)siloxane	
1b	99 (99, 99, 99, 99, 99, 99, 99, 99, 99)

Reaction conditions—[SiH]:[H$_2$C=CHR]:[Rh] = 1:1.5:10^{-4}, T = 100 °C, 1 h, open system, glass ampoules, argon.
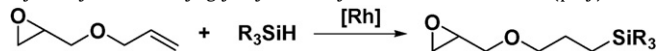
with heptamethyltrisiloxane (HMTS) even after 21 runs (Fig. 6). Rhodium content in the sample of the catalyst **1b**, determined by ICP-OES, used for 20 cycles in this process was 0.16 mmol/g, which makes 72% of the initial amount of rhodium in catalyst **1b**.

While comparing catalytic performance of Aerosil-supported rhodium siloxide complex (**1**) with that of SBA-15-supported one (**2**), the former catalyst proved to be better, which can

Table 5

Hydrosilylation of allyl glycidyl ether by substituted silanes and (poly)siloxanes.

Cat.	Yield (%)
Triethoxysilane	
1b	94 (94, 94, 93, 92, 89, 76, 62, 34, 23)
2	94 (92, 89, 92, 70, 19)
3	95
Heptamethyltrisiloxane	
1b	94 (TOF = 156 min^{-1}) (94, 94, 94, 92, 89, 77, 62, 33, 23)
3	94
4	94 (99, 97, 95, 95, 95, 64, 51, 44, 37)
Poly(hydro,methyl)(dimethyl)siloxane	
1b	99 (99, 99, 99, 95, 91, 85, 83, 75, 55)
3	99

Reaction conditions—[SiH]:[H$_2$C=CHR]:[Rh] = 1:1.5:10^{-4}, T = 100 °C, 1 h, open system, glass ampoules, argon.

be most clearly seen in the case of hydrosilylation of vinyl-heptamethyltrisiloxane by heptamethyltrisiloxane. Since Aerosil 200 is nonporous, one can speculate that the reason for better performance of the Aerosil-based catalyst is easier access of reactants to active centers, whereas a possibility of diffusion retardation could be considered in the case of porous SBA-15-based catalyst. However, such an interpretation has to be ruled out when mean pore size of SBA-15 (which is 6 nm) is compared to the size of activated complex. Geometry of the latter was roughly evaluated by using the UFF (universal force field) method [41] and the size of the activated complex appeared to be about 1 nm, when measured from oxygen atom in Si–O–Rh to the most distant hydrogen atom in vinylheptamethyltrisiloxane (Fig. 7).

Even if another molecule of active complex is located just on the opposite wall of SBA-15 pore, the latter becomes narrower by 2 nm, which means that as much as 4 nm of unhindered space is still available. Therefore, the reason for poorer performance of SBA-15-supported catalyst must be different. Most likely it should be sought in a greater extent of rhodium leaching from the latter catalyst. Surface coverage with silanol groups is smaller on SBA-15 than on Aerosil 200, which can result in the possibility that some molecules of di-μ-trimethylsiloxybis{(1,5-cyclooctadiene)rhodium(I)} present in the pores of SBA-15 are not immobilized by surface OH groups, and such unanchored species are vulnerable to leaching. This is, most likely, why in the reaction between vinylheptamethyltrisiloxane and heptamethyltrisiloxane the decrease in the yield from about 90% to about 58% (Table 3) is accompanied by reduction in rhodium content in SBA-15-based catalyst to 51% of the initial Rh content (compared to 72% in the case of Aerosil-supported catalyst).

Table 6

Percentage of initial rhodium content (determined by ICP-OES technique) in catalysts after hydrosilylation reactions.

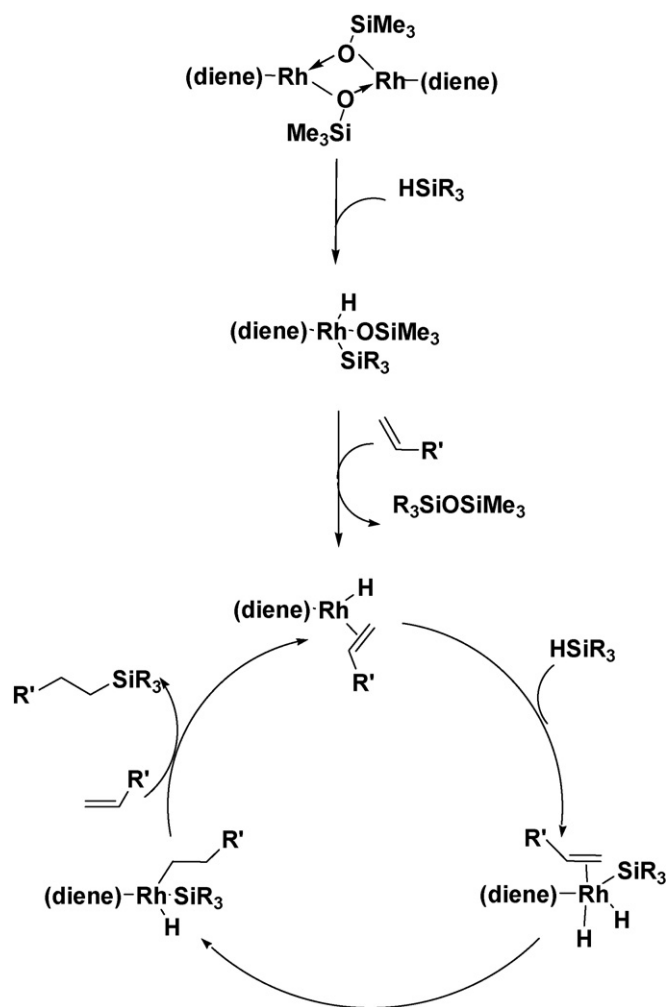| Catalyst	Initial loading (mol Rh/g)	After hydrosilylation of		
		1-C$_{16}$H$_{32}$ with HMTS	VHMTS with HMTS	AGE with HMTS
1a	2.17 × 10^{-4}		50%	
1b	4.10 × 10^{-4}	70%	72%	50%
2	8.13 × 10^{-4}		51%	
3	2.32 × 10^{-4}		47%	
4	5.00 × 10^{-4}	23%	29%	9%

Fig. 8. Mechanism of homogeneous catalysis of alkene hydrosilylation by [{Rh(μ-OSiMe$_3$)(cod)}$_2$].

Rhodium immobilized complexes were found to be effective catalysts for the addition of HSi(OEt)$_3$, HSiMe(OSiMe$_3$)$_2$ and poly(hydro,methyl)(dimethyl)siloxane to various allyl ethers. The data presented in Tables 4 and 5 confirm high catalytic activity of all catalysts used in the reactions studied, but only in the case of allyl phenyl ether, particularly in the reaction with siloxane and polysiloxane, the catalytic activity remained unchanged up to 10 cycles (Table 4). In the hydrosilylation of allyl glycidyl ether (AGE), products of which (epoxy-functionalized silanes and (poly)siloxanes) are commercially available, we have observed a

decrease in catalytic activity of catalyst **1** after 7–9 runs. Results of ICP-OES analysis of rhodium siloxide catalysts after 10 catalytic runs proved that rhodium content was still relatively high. Therefore, the decrease in the activity of catalyst **1** was, probably, caused not only by rhodium leaching from the catalyst.

Data presented in Table 6 lead to conclusion that the complex **4** is the most susceptible to leaching from among all catalysts studied. This suggests a considerably weaker interaction between the complex and silica surface. Particularly high leaching was observed in the case hydrosilylation of allyl glycidyl ether (AGE) with heptamethyltrisiloxane (HMTS) which resulted in the removal of 98% of the initial amount of rhodium present in the catalyst **4**. However, it is worth to add that the latter reaction caused changes also in other catalysts and the changes were not limited to rhodium leaching only. Both post-reaction mixtures and catalysts assumed dark color after each repetition of the reaction. Presumably this is a result of deactivation of the complexes by allyl glycidyl ether.

As we have previously proved, catalysis of hydrosilylation by dimeric (as well as by monomeric) rhodium siloxide complexes proceeds via initial oxidative addition of silicon hydride followed by elimination of disiloxane (detected by GC–MS) to generate the square planar 16e hydride complex with already coordinated molecule of alkene (see Fig. 8).

The latter complex initiates the catalytic cycle for hydrosilylation of olefins to be a key intermediate in all catalytic transformations with rhodium siloxide complexes, such as silylcarbonylation and hydroformylation [23]. If such an initial 16e Rh–H complex, containing no siloxide ligand, was formed also in the immobilized catalyst, then the leaching of rhodium complex should be observed. However, results of solid-state NMR measurements have shown the presence of surface siloxide complex ≡SiORh(H)Si (**5**) identified as a product of the oxidative addition of dimethylphenylsilane to the initial complex **1** [27] (Fig. 9).

The absence of the disiloxane elimination in this system is an additional evidence for formation of such a key intermediate in the heterogeneous system. Therefore, the catalytic cycle of the hydrosilylation by **1–4,** e.g. **1,** have to be different from that of the homogeneous one and should involve a catalytic pathway protecting the surface-siloxide intermediates against leaching during the whole cycle. Apparently, the reaction proceeds via the well-known Chalk-Harrod mechanism initiated by the stable immobilized ≡SiORh(I)(diene) complex. The process of the oxidative addition of silicon hydride to **1** was proved by NMR study. The subsequent coordination of alkene to the surface-siloxide rhodium complex is followed by its insertion into Rh–H bond with final elimination of the hydrosilylation product and regeneration of the stable surface rhodium-siloxide species **1**. The interaction of surface silanol groups in **1** seems to be responsible for the high stability of such a single-site rhodium catalyst, which can be recycled for at least 10–20 times without a decrease in the high yield and selectivity (Fig. 10).
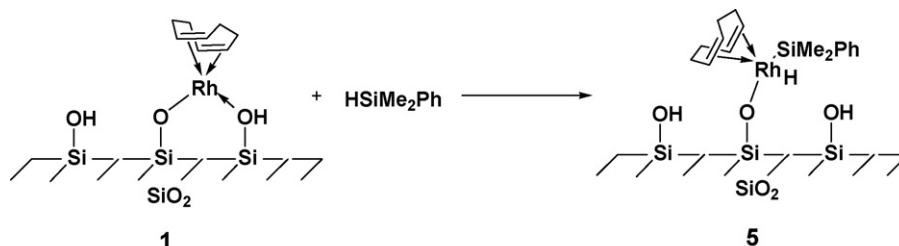

Fig. 9. Reaction of oxidative addition of dimethylphenylsilane to the initial complex **1**.
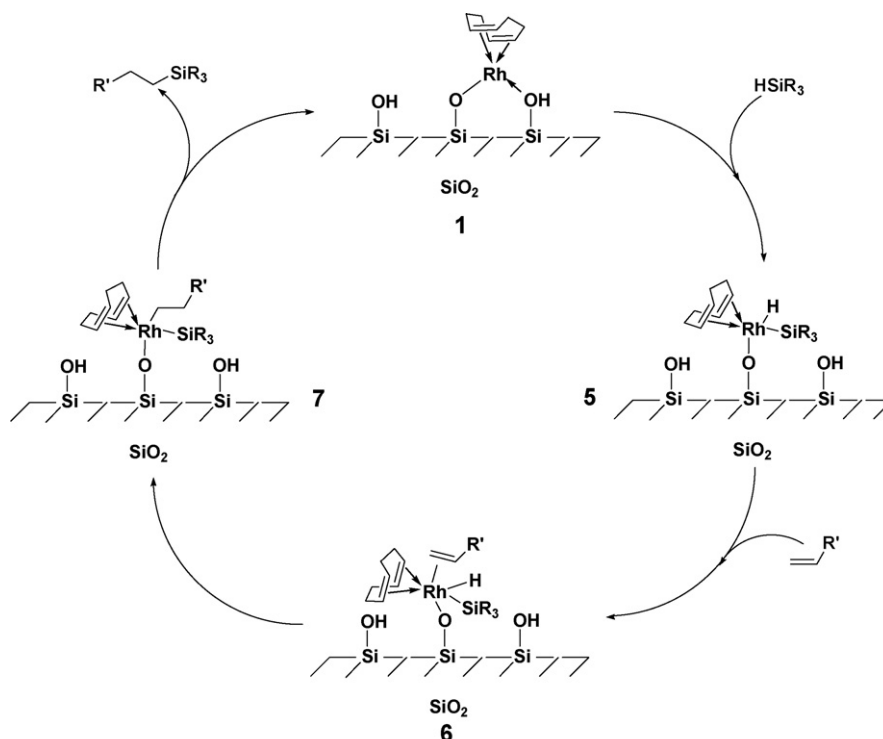
Fig. 10. Mechanism of heterogeneous catalysis of hydrosilylation by surface rhodium(diene)siloxide complex.

4. Conclusions

Well-defined surface siloxide rhodium complexes (**1**–**4**) can be used as very attractive catalysts for commercially important syntheses via hydrosilylation, particularly for the modification of (poly)siloxanes.

We wish to stress that the characterization of complex **5** by solid-state NMR spectroscopy as well as by analysis for rhodium content after 10–20 cycles provides with a convincing evidence for high efficiency of surface rhodium siloxide complexes in the hydrosilylation of carbon–carbon multiple bond, as well as presumably in other reactions catalyzed by rhodium and other late transition metal siloxide complexes synthesized via direct reaction of molecular late transition metal siloxide precursors with silica.

References

[1] B. Marciniec, H. Maciejewski, Coord. Chem. Rev. 223 (2001) 301–335.
[2] F.J. Feher, T.A. Budzichowski, Polyhedron 14 (1995) 3239–3253.
[3] P.T. Wolczanski, Polyhedron 14 (1995) 3335–3362.
[4] F.J. Feher, R.L. Blanski, J. Am. Chem. Soc. 114 (1992) 5886–5887.
[5] F.J. Feher, T.L. Tajima, J. Am. Chem. Soc. 116 (1994) 2145–2146.
[6] A. Choplin, B. Coutant, C. Dubuisson, P. Leyrit, C. McGill, F. Quignard, R. Teissier, Stud. Surf. Sci. Catal. 108 (1997) 353–360.
[7] L.D. Ornelos, A. Choplin, J.M. Basset, L.Y. Hsu, S. Shore, Nouv. J. Chim. 9 (1985) 155.
[8] J. Vizi-Orosz, R. Ugo, R. Psaro, A. Sironi, M. Moret, C. Zuchi, F. Ghelfi, G. Palyi, Inorg. Chem. 33 (1994) 4600–4603.
[9] N. Kornev, T.A. Chesnokova, V.V. Semenov, E.V. Zhezlova, L.N. Zakhonov, L.G. Klapshina, G.A. Domrachev, V.S. Rusakov, J. Organomet. Chem. 547 (1997) 113–119.
[10] B. Marciniec, P. Krzyżanowski, M. Kubicki, Polyhedron 15 (1996) 4233–4239.
[11] B. Marciniec, P. Krzyżanowski, J. Organometal. Chem. 493 (1995) 261–266.
[12] B. Marciniec, P. Błażejewska-Chadyniak, M. Kubicki, Can. J. Chem. 81 (2003) 1292–1298.
[13] B. Marciniec, I. Kownacki, M. Kubicki, Organometallics 21 (2002) 3263–3270.
[14] I. Kownacki, M. Kubicki, B. Marciniec, Inorg. Chim. Acta 334 (2002) 301–307.
[15] I. Kownacki, B. Marciniec, M. Kubicki, Chem. Commun. 1 (2003) 76–77.
[16] B. Marciniec, P. Krzyżanowski, E. Walczuk-Guściora, W. Duczmal, J. Mol. Catal. A: Chem. 144 (1999) 263–271.
[17] B. Marciniec, P. Błażejewska-Chadyniak, I. Kownacki, K. Szubert, Pol. Pat. Apl. P-368 485 (2004).
[18] B. Marciniec, E. Walczuk, P. Błażejewska-Chadyniak, D. Chadyniak, M. Kujawa-Welten, S. Krompiec, Organosilicon Chemistry V - from Molecules to Materials, Verlag Chemie, 2003.
[19] B. Marciniec, P. Błażejewska-Chadyniak, E. Walczuk-Guściora, M. Kujawa-Welten, Pol. Pat. 194667 (2001).
[20] B. Marciniec, in: A.M. Trzeciak (Ed.), Perspectives of Coordination Chemistry, Poznań-Wrocław, 2005, pp. 195–214.
[21] B. Marciniec, E. Walczuk-Guściora, P. Błażejewska-Chadyniak, J. Mol. Catal. A: Chem. 160 (2000) 165–171.
[22] B. Marciniec, E. Walczuk-Guściora, C. Pietraszuk, Organometallics 20 (2001) 3423–3428.
[23] E. Mieczyńska, A.M. Trzeciak, J.J. Ziółkowski, I. Kownacki, B. Marciniec, J. Mol. Catal. A: Chem. 237 (2005) 246–253.
[24] A. Theolier, A.K. Smith, M. Leconte, J.M. Basset, G.M. Zanderighi, R. Psaro, R. Ugo, J. Organomet. Chem. 191 (1980) 415–424.
[25] P. Dufour, C. Houtman, C.C. Santini, C. Nedez, J.M. Basset, L.Y. Hsu, S.G. Shore, J. Am. Chem. Soc. 114 (1992) 4248–4257.
[26] C.C. Santini, S.L. Scott, J.M. Basset, J. Mol. Catal. 107 (1996) 263–271.
[27] B. Marciniec, K. Szubert, M.J. Potrzebowski, I. Kownacki, K. Łęszczak, Angew. Chem. Int. Ed. 47 (2008) 541–544.
[28] B. Marciniec, K. Szubert, K. Łęszczak, I. Kownacki, R. Fiedorow, M. Dutkiewicz, PCT/PL2007/000064 (2007).
[29] B. Marciniec, K. Szubert, M. Dutkiewicz, I. Kownacki, R. Fiedorow, Pol. Pat. Appl. P-380 621 (2006).
[30] B. Marciniec, H. Maciejewski, C. Pietraszuk, P. Pawluć, Hydrosilylation. A Comprehensive Review on Recent Advances, B. Marciniec (Ed.), Springer, London, 2008, [http://www.springer.com/chemistry].
[31] B. Marciniec, P. Krzyżanowski, J. Organometal. Chem. 493 (1995) 261.
[32] For complex [{Rh(μ-OSiMe₃)(tfb)}₂], K. Szubert, I. Kownacki, B. Marciniec, unpublished data.
[33] C.R. Morcombe, K.W. Zilm, J. Magn. Reson. 162 (2003) 479–486.
[34] G. Metz, X. Wu, S.O. Smith, J. Magn. Reson. Ser. A 110 (1994) 219–227.
[35] A.W. Bennett, C.M. Rienstra, M. Auger, K.V. Lakshmi, R.G. Griffin, J. Chem. Phys. 103 (1995) 6951–6958.
[36] D. Zhao, Q. Huo, J. Feng, B.F. Chmelka, G.D. Stucky, J. Am. Chem. Soc. 120 (1998) 6024–6036.
[37] C. Okkerse, in: B.G. Linsen (Ed.), Physical and Chemical Aspects of Adsorbents and Catalysts, Academic Press, London/New York, 1970, pp. 258–259.
[38] B. Marciniec, K. Szubert, A. Franczyk, I. Kownacki, R. Fiedorow, Pol. Pat. Apl. P-381 555 (2007).
[39] B. Marciniec, K. Szubert, A. Franczyk, I. Kownacki, R. Fiedorow, Pol. Pat. Apl. P-381 556 (2007).
[40] B. Marciniec, K. Szubert, K. Łęszczak, I. Kownacki, Pol. Pat. Apl. P-383 213 (2007).
[41] A.K. Rappe, C.J. Casewit, K.S. Colwell, W.A. Goddard III, W.M. Skiff, J. Am. Chem. Soc. 114 (1992) 10024–10035.